# Magnetic ordering in the kagomé lattice antiferromagnet $KCr_3(OD)_6(SO_4)_2$

T. Inami
*Synchrotron Radiation Research Center, Japan Atomic Energy Research Institute, Mikazuki, Hyogo 679-5148, Japan*

T. Morimoto, M. Nishiyama, and S. Maegawa
*Graduate School of Human and Environmental Studies, Kyoto University, Kyoto 606-8501, Japan*

Y. Oka
*Faculty of Integrated Human Studies, Kyoto University, Kyoto 606-8501, Japan*

H. Okumura
*Institute for Solid State Physics, University of Tokyo, Roppongi 7-22-1, Minato-ku, Tokyo 106, Japan*
(Received 12 October 2000; revised manuscript received 7 February 2001; published 17 July 2001)

Measurements of the magnetic susceptibility and neutron powder diffraction revealed that the kagomé lattice antiferromagnet $KCr_3(OD)_6(SO_4)_2$ exhibits clear long-range magnetic order at $T_N = 4.0$ K in contrast to previous reports. The ordered magnetic structure is found to be the so-called $q=0$ type 120° structure on the kagomé lattice. A model which satisfies the observed magnetic intensity is, however, that the direction of the ordered moments, which form a nearly coplanar 120° ground state, distribute uniformly in the *ab* plane. We propose a $q=0$ structure fluctuating slowly around the *c* axis as a ground state. This explanation may give a reasonable account for the obtained magnetic structure and the sample dependence.

DOI: 10.1103/PhysRevB.64.054421 PACS number(s): 75.25.+z

## I. INTRODUCTION

Heisenberg spins on a kagomé lattice coupled with antiferromagnetic nearest-neighbor interactions have attracted considerable attention, because the system does not have conventional magnetic long-range order due to the infinite number of the degenerate ground states. Theoretically, several ground states have been investigated including two states consisting of 120° spin arrangements, the $q=0$ structure [Figs. 1(a) and 1(b)] and the $\sqrt{3}\times\sqrt{3}$ structure [Fig. 1(c)]. These studies suggest that the degeneracy might be lifted by thermal[1,2] and quantum[3] fluctuations and that the $\sqrt{3}\times\sqrt{3}$ structure is favored as the ground state, whereas exotic magnetic ground states such as nematic order are also expected.[4]

The alunite family of compounds of the general formula $AM_3(OH)_6(SO_4)_2$ (*A*: monovalent ion $Na^+$, $K^+$, $Rb^+$, $Tl^+$, $Ag^+$, $NH_4^+$, *M*: trivalent ion $Al^{3+}$, $Fe^{3+}$, $Cr^{3+}$, $Ga^{3+}$) has a kagomé lattice in the *ab* plane, as seen in Fig. 2. The $M^{3+}$ ions, which are coordinated by two O(2) oxygen atoms and four O(3) oxygen atoms, reside at the vertices of the kagomé lattice. The neighboring $MO_6$ octahedra share an O(3) oxygen atom at the corner. The kagomé layers are well separated by nonmagnetic $A^+$ ions and $SO_4^{2-}$ groups. Therefore, when $M^{3+}$ is a magnetic ion, the compound is expected to be a good candidate for a two-dimensional kagomé lattice antiferromagnet.

Our recent study of the alunite-type compound $KFe_3(OH)_6(SO_4)_2$ (K jarosite) has revealed interesting features of this class of compounds.[5] A remarkable feature of alunite-type magnets is that anisotropy can play an important role in selecting the ground state. As opposed to an ideal kagomé lattice Heisenberg antiferromagnet, K jarosite undergoes long-range magnetic order below 65 K. The prominent point is that the magnetic structure consists of the $q=0$ structure with $+1$ chirality only [Fig. 1(a)], where the chirality is defined as $+1$ and $-1$ when the spins rotate by 120° clockwise and counter-clockwise, respectively, as one traverses around the triangle clockwise. In addition, the values of $\phi$, the angle between the spin 1 and the *b* axis [see Fig. 1(a)], are fixed at $\pm 90°$ only. Note that isotropic exchange interactions give the same ground-state energy for both the $q=0$ structure with $+1$ chirality and one with $-1$ chirality [Fig. 1(b)]. The observed selection is due to the single-ion-type anisotropy of the $Fe^{3+}$ ion. Since the magnetic $Fe^{3+}$ ion is surrounded by an oxygen octahedron with orthorhombic distortion, the anisotropy is represented by both *D* and *E* in the spin Hamiltonian, which is

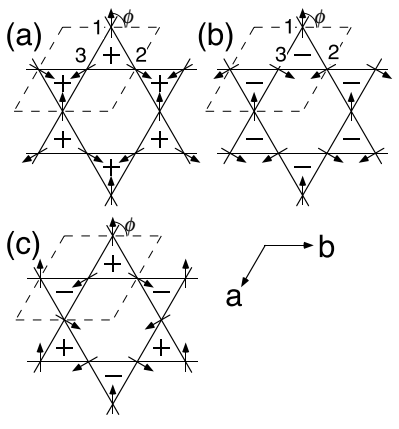


FIG. 1. (a) the $q=0$ structure with chirality $+1$, (b) the $q=0$ structure with chirality $-1$, (c) the $\sqrt{3}\times\sqrt{3}$ structure. The broken line shows the unit cell of a kagomé lattice. The $+$ and $-$ signs at the center of a triangle indicate that the triangle of the spins has $+1$ and $-1$ chirality, respectively.

 

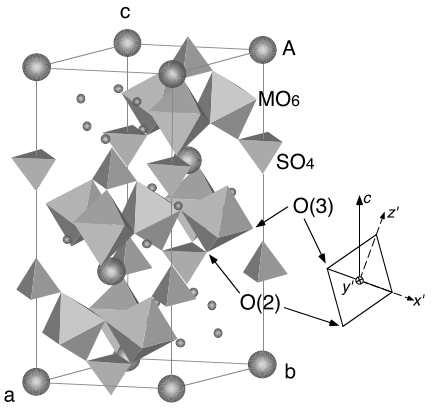


FIG. 2. Crystal structure of $AM_3(OH)_6(SO_4)_2$. Octahedra and tetrahedra indicate $MO_6$ and $SO_4$ groups, respectively. Note that the principal axis of the octahedron O(2)-*M*-O(2) is not parallel to the *c* axis.

$$\mathcal{H}=-2J\sum_{\langle i,j\rangle}\mathbf{S}_i\cdot\mathbf{S}_j-D\sum_i(S_i^{z'})^2-E\sum_i\{(S_i^{x'})^2-(S_i^{y'})^2\}, \tag{1}$$

where $J$ is isotropic exchange constant in the kagomé plane. The $z'$ and $y'$ axes are taken to be parallel to the O(2)-Fe-O(2) axis and to be in the *ab* plane, respectively, for each site. Note that the $z'$ axes are *not* parallel to the *c* axis. Consider that the anisotropy is easy-plane type ($D<0$), because the ordered moment was found to lie (mostly) in the *ab* plane in K jarosite. The ground state is predominantly the coplanar 120° structure, because it is thought that $|J|\gg|D|$ and $|E|$. However, the $x'$ axes are not in the same plane. When thereby $E$ is positive ($x'$ is easy axis), competition between $J$ and $E$ occurs. As a result, when $E\gtrsim|D|\sin^2\alpha/(1+\cos^2\alpha)$, where $\alpha$ is the angle between the *c* axis and the $z'$ axis, the $q=0$ structure with $+1$ chirality of $\phi=+90°$ ($-90°$) is the ground state, otherwise the $q=0$ structure with $+1$ chirality of $\phi=0°$ (180°) is selected. The former is the magnetic structure observed in the K jarosite; the anisotropy selects the ground state. Another interesting feature is that in the magnetic structure of the K jarosite the ordered moments are slightly canted from the complete coplanar 120° structure in the *ab* plane to each $x'$ axis similar to an umbrella in order to gain the anisotropy energy. The net moment of each umbrella cumulates and gives rise to a net moment for a kagomé plane. In K jarosite, it stacks in an alternate manner along the *c* axis and does not give rise to a net moment for a whole crystal.

$KCr_3(OH)_6(SO_4)_2$ is a kagomé lattice antiferromagnet of $S=\frac{3}{2}$ which belong to the alunite-type compounds. Magnetic susceptibility data were fitted using a Curie-Weiss law with the Curie-Weiss constant $\Theta_{CW}=-67.5\,K$ and a low-temperature part of the data suggests magnetic ordering at $T_N\sim2\,K(\ll\Theta_{CW})$.[6] Keren *et al.* have shown that the history dependence indeed appears in the magnetic susceptibility below $T_N$ and, nevertheless, they found that a strong dynamic spin fluctuation remains even at $T=25\,mK$ in the $\mu$SR measurement.[7] Neutron diffraction measurements revealed that long-range magnetic order exists below $T_N=1.8\,K$. The ordered moment, however, was found to be only $1.1\mu_B$ per Cr site ($\langle S\rangle/S=0.4$) and the inelastic neutron scattering measurements showed that most of the chromium spin remains dynamic far below $T_N$.[8] All these results indicate that the ground state of $KCr_3(OH)_6(SO_4)_2$ has strong spin fluctuations.

In the present paper, we report on magnetic ordering in $KCr_3(OD)_6(SO_4)_2$, which we investigated by means of magnetic susceptibility and neutron powder diffraction. In contrast to the previous reports, $KCr_3(OD)_6(SO_4)_2$ with 95% occupancy of the chromium site shows a sharp rise in susceptibility at $T_N=4.0\,K$, indicating a definite magnetic transition and weak ferromagnetism. The antiferromagnetic structure obtained from neutron diffraction data at 1.7 K is the $q=0$ structure in accordance with the previous report.[8] However, quantitative analysis showed that the system is divided into a number of domains in which the ordered moments that make the 120° spin arrangement point to various direction (mostly) in the *ab* plane. A possible model which may explain the observed domain structure is proposed. In this model, $KCr_3(OD)_6(SO_4)_2$ is considered as an *XY*-spin system and slow fluctuation around the *c* axis exists in the ground state.

## II. EXPERIMENTAL DETAILS

The deuterated $KCr_3(OD)_6(SO_4)_2$ powder sample was synthesized by a hydrothermal reaction. The starting materials $K_2SO_4$ and $Cr_2(SO_4)_3$ were mixed in 99.75% $D_2O$, and heated in a Pyrex ampule at 280 °C for 55 h using an autoclave. The $Cr_2(SO_4)_3$ was dehydrated prior to use in order to avoid contamination of the hydrogen. The obtained gray precipitation was washed with hot water and dried. X-ray powder diffraction analysis showed that the sample has a single phase. The typical crystalline size of the sample was a few $\mu$m from the SEM observation. The occupancy of the chromium site is estimated to be 95% from neutron diffraction data, as shown later, and the partial substitution of $D_3O^+$ for $K^+$ is also indicated.

Bulk susceptibility data were measured between 2 and 300 K on warming under a magnetic field 500 Oe using a SQUID magnetometer (Quantum Design MPMS2). Neutron powder diffraction data were collected on the high resolution powder diffractometer HRPD and the triple axis spectrometer TAS-2 operated at the research reactor JRR-3M, JAERI (Tokai). The high-resolution data were collected on the HRPD using a wavelength of 1.16271 Å at 300 K to refine the structural parameters. The medium-resolution data were measured on the TAS-2 with a two-axis mode at 1.7 and 10 K using a wavelength of 2.443 Å, and were used to determine the magnetic structure. The temperature evolution of the magnetic Bragg reflection {012} was also measured on the TAS-2. The sample was placed in a cylindrical vanadium can of 10 mm in diameter with $^4$He exchange gas and cooled using an ILL ''orange'' liquid helium cryostat. The diffraction patterns were analyzed by the Rietveld method using the program RIETAN.[9,10] In the refinements, the background was fitted with a 12-term polynomial and a 6-term polynomial for

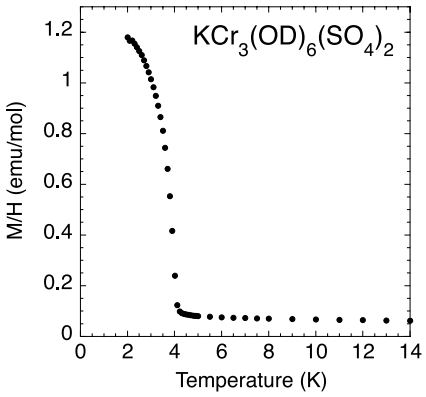


FIG. 3. Zero-field-cooled susceptibility of $KCr_3(OD)_6(SO_4)_2$ as a function of temperature.

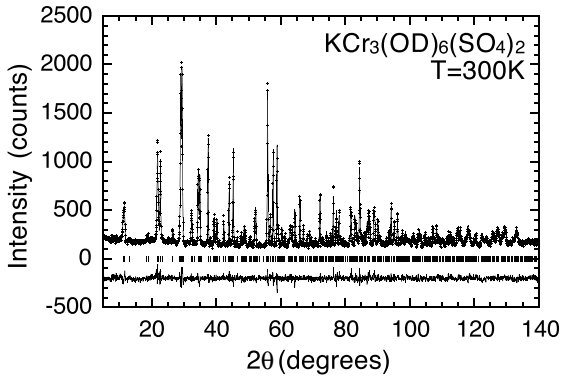


FIG. 4. A Rietveld plot of $KCr_3(OD)_6(SO_4)_2$ neutron-powder diffraction data at 300 K. The experimental points are indicated as crosses. The solid line is the calculated fit to the pattern. A difference curve is plotted at the bottom. The tick marks indicate the position of the Bragg reflections.

the high-resolution data and the medium-resolution data, respectively, and a pseudo-Voigt peak shape function was employed.

### III. RESULTS AND DISCUSSION

The studies on the magnetic properties of $KCr_3(OH)_6(SO_4)_2$ investigated so far indicate that $KCr_3(OH)_6(SO_4)_2$ has no long-range order[7] or that the order is at most very weak.[8] However, the susceptibility data of our sample give a clear indication of the presence of a sharp magnetic phase transition.[11] In Fig. 3, the susceptibility is plotted as a function of temperature in the low-temperature part. A small spontaneous magnetic moment appears suddenly below the Neél temperature $T_N = 4.0\,\mathrm{K}$, indicating a magnetic phase transition into an antiferromagnet with a slightly canted moment. This anomaly does not stem from ferromagnetic impurity, as will be shown later in neutron diffraction data. Except this spontaneous moment, the susceptibility agrees very well with the reported result.[6] Detailed quantitative analysis of the susceptibility of $ACr_3(OH)_6(SO_4)_2$ (*A*: Alkaline metals) including this sample up to 300 K will be published elsewhere.[12]

The quality of the sample was examined using high-resolution neutron powder diffraction data. Rietveld refinements were carried out in space group $R\bar{3}m$ and the result of the refinements is shown in Fig. 4. All thermal parameters and occupancy of the Cr site were refined. The obtained structural parameters are presented in Table I and are in good agreement with the previously reported values.[8,13] The partial substitution of hydrogen for deuterium does not yield a marked improvement in the fit. Thus, combined with the observed low background in neutron diffraction data, we assumed that the D site is fully occupied by deuterium. The refinement of the occupancy of the K site resulted in an occupancy much larger than 100%. During the course of the refinements, thus we fixed the occupancy of the K site at unity. This is probably due to the substitution of $D_3O^+$ for $K^+$,[13,14] and the large isotropic thermal parameter for the K site also appears to indicate medium structural disorder at the K site. The occupancy of the Cr site is $95\pm3\%$ and is consistent with the value estimated from magnetic susceptibility $86\pm1\%$;[12] it seems that the Cr site is slightly deficient.

Neutron powder diffraction data measured at 10 and 1.7 K are shown in Fig. 5. At 1.7 K, a series of magnetic Bragg reflections are observed. All the magnetic peaks can be indexed using a magnetic unit cell identical to the chemical one. The temperature evolution of the peak intensity for {012} magnetic reflection shown in Fig. 6 illustrates that the

TABLE I. Structure parameters of $KCr_3(OD)_6(SO_4)_2$ at 300 K as derived from the Rietveld refinement. Standard deviations for refined values are given in parentheses. Space group $R\bar{3}m$ in hexagonal setting ($Z=3$). $B_{iso}$ is the isotropic thermal parameter.

$a = 7.2225(2)$ Å $\quad c = 17.2122(5)$ Å
$R_{wp} = 8.27\%$ $\quad R_{exp} = 6.63\%$ $\quad R_F = 2.47\%$

| atom | site | occupancy | *x* | *y* | *z* | $B_{iso}$/Å$^2$ |
|---|---|---|---|---|---|---|
| K | 3*a* | 1.0 | 0.0 | 0.0 | 0.0 | 1.4(2) |
| Cr | 9*d* | 0.95(3) | 0.5 | 0.5 | 0.5 | 0.4(1) |
| S | 6*c* | 1.0 | 0.0 | 0.0 | 0.3045(6) | 0.2(1) |
| O(1) | 6*c* | 1.0 | 0.0 | 0.0 | 0.3888(4) | 0.6(1) |
| O(2) | 18*h* | 1.0 | 0.2217(3) | −0.2217 | −0.0574(2) | 0.6(1) |
| D | 18*h* | 1.0 | 0.1962(3) | −0.1962 | 0.1105(2) | 1.7(1) |
| O(3) | 18*h* | 1.0 | 0.1277(3) | −0.1277 | 0.1356(2) | 0.6(1) |

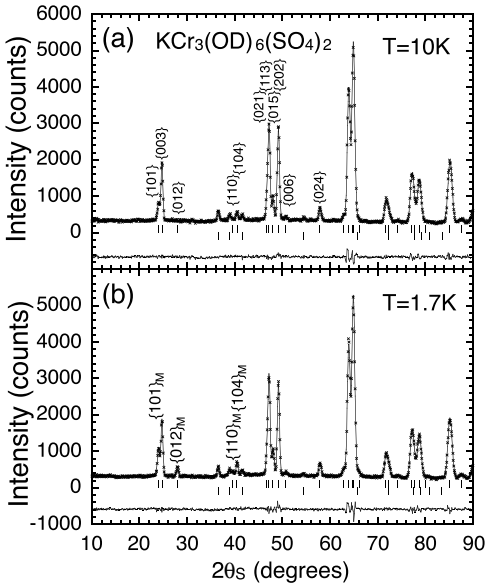


FIG. 5. A Rietveld plot of $KCr_3(OD)_6(SO_4)_2$ neutron-powder diffraction data at 10 K (a) and 1.7 K (b). The plot at 1.7 K was fitted using the magnetic structure described in the text. The notation is as in Fig. 4 except the tick marks. The tick marks (top) represent the position of nuclear and magnetic Bragg reflections for $KCr_3(OD)_6(SO_4)_2$, while the tick marks (bottom) indicate Bragg reflections for an impurity phase (solid heavy water). The Bragg reflections which have magnetic intensity are indexed with a mark *M* in (b).

transition temperature is actually 4.0 K and that the spontaneous moment observed in the susceptibility data definitely arises from the magnetic ordering of $KCr_3(OD)_6(SO_4)_2$.

Since the observed magnetic reflections fulfill the reflection condition $-h+k+l=3n$ ($n$: integer), the magnetic unit cell is a rhombohedral one, and thus there are three independent magnetic moments in the unit cell. No large net moment in the ordered phase is detected in magnetization measurements ($0.14\mu_B/Cr^{3+}$),[12] thus the most plausible magnetic structure is the so-called 120° structure, in which the neighboring spins make an angle of 120°, because this is the easiest way for the moments to cancel each other. The obtained

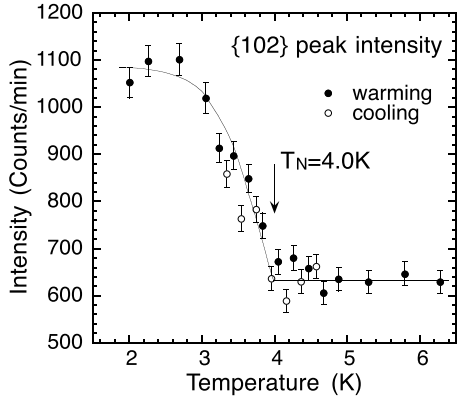


FIG. 6. Development of the peak intensity of the magnetic reflection {012} as a function of temperature.

TABLE II. Observed integrated intensities of magnetic Bragg peaks and squared magnetic structure factors for the several models. (−: chirality −1; 90, 60, 45, 30, and 0: chirality +1 with $\phi=90°$, 60°, 45°, 30°, and 0°, respectively.) Lorentz factors and magnetic form factors are corrected for $I_{obs}$. $R$ factors are also shown in the last row. The best fits are obtained for the models with chirality −1 and with chirality +1 of $\phi=45°$. $R=\Sigma|I_{obs}-I_{calc}|/\Sigma I_{obs}$, $I_{calc}\propto m_{hkl}|F_M|^2$, $m_{hkl}$: multiplicity.

| | | $\lvert F_M\rvert^2$ | | | | | | |
|---|---|---|---|---|---|---|---|---|
| | | Chirality | −1 | | | +1 | | |
| *hkl* | $I_{obs}$ | $\phi$ | − | 90 | 60 | 45 | 30 | 0 |
| 101 | 14.2(1.5) | | 20.1 | 4.24 | 12.2 | 20.1 | 28.1 | 36 |
| 012 | 19.0(2.2) | | 24.3 | 12.5 | 18.4 | 24.3 | 30.1 | 36 |
| 110 | 11.5(4.3) | | 18 | 36 | 27 | 18 | 9 | 0 |
| 104 | 19.6(4.5) | | 30.3 | 24.5 | 27.4 | 30.3 | 33.1 | 36 |
| $R$(%) | | | 7.2 | 57.7 | 29.7 | 7.2 | 15.2 | 26.3 |

magnetic structures correspond to the $q=0$ structures shown in Figs. 1(a) and 1(b). As we observed before in the K jarosite, in alunite-type compounds the anisotropy favors the $q=0$ structure with chirality +1 of $\phi=0°$ or 90°, depending on the sign and magnitude of the anisotropy $E$[5]. However, for $KCr_3(OD)_6(SO_4)_2$, the observed magnetic intensities could not be accounted for by these two models. We present the measured and calculated integrated intensities of the magnetic Bragg peaks in Table II. The calculated models are the *ab* plane $q=0$ structures with chirality +1 and with chirality −1. The structure factors for the *ac* plane $q=0$ structure did not fit the observed intensities, thus the anisotropy $D$ is considered to be easy plane type. Since the structure factor is a function of $\phi$ for the $q=0$ structure with chirality +1, we calculated it for several values of $\phi$. On the other hand, the structure factor for the $q=0$ structure with chirality −1 is independent of $\phi$. The moments are assumed to lie in the *ab* plane in the calculation because the ferromagnetic moment is very small. The best fit is obtained for the models with chirality −1 and with chirality +1 of $\phi=45°$, as seen in $R$ factors in Table II.

As mentioned above, the spin Hamiltonian (1) has only two ground states, $q=0$ structures with chirality +1 of $\phi=90°$ and 0°, thus this result can not be accepted. In fact, there is another model which reproduces the magnetic intensity observed in diffraction data. The calculated intensities for the $q=0$ structure with chirality +1 are proportional to $A+B\cos^2\phi$. Therefore the squared magnetic structure factor $|F_M|^2$ averaged about $\phi(=A+\frac{1}{2}B)$ is equal to that for the above two models (the $q=0$ structures with chirality −1 and with chirality +1 of $\phi=45°$). This corresponds to the following magnetic structure. The whole system consists of a number of domains, each of which has the long-range ordered $q=0$ structure with chirality +1 of an arbitrary value of $\phi$, and the value of $\phi$ distributes randomly among the domains. The width of the magnetic Bragg peaks is limited by instrumental resolution, thus the antiferromagnetic correlation length of each domain is estimated to exceed about

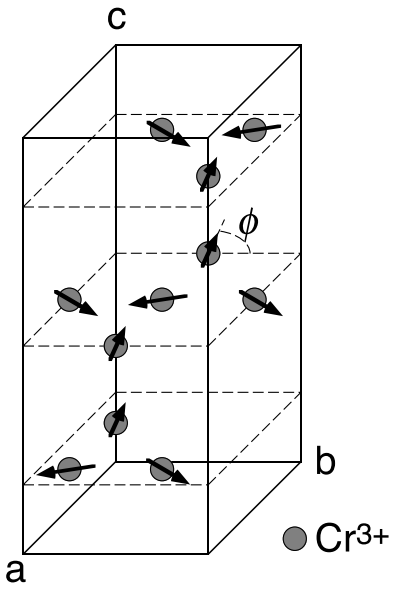


FIG. 7. Proposed magnetic structure below $T_N$. The ordered moments are shown by arrows and slightly cant from the basal plane. The angle between the moment and the *b* axis ($\phi$) in a domain is different from other domains.

400 Å. Each triangle of the moments probably cants in order to satisfy anisotropy terms and produces a small net moment out of the kagomé plane, as is the case in K jarosite.[5] For the magnetic structure of $KCr_3(OD)_6(SO_4)_2$, the net moment stacks ferromagnetically and, consequently, the small spontaneous moment arises, which is observed in the susceptibility measurement. We will discuss this model in detail below. Rietveld refinement using this model readily converged to $R_{wp}=5.33\%$ ($R_{exp}=4.21\%$), $R_{I(nuclear)}=1.29\%$ and $R_{I(magnetic)}=3.38\%$. The result of the refinement is shown in Fig. 5(b). None of the isotropic thermal parameters were refined and the occupancy factors were fixed at unity, because the measured *Q* range is not wide enough to refine those parameters reliably. The ordered moment evaluated from the refinement is $1.98(8)\mu_B/Cr^{3+}$. The magnetic structure of $KCr_3(OD)_6(SO_4)_2$ is shown in Fig. 7.

The specific features of the magnetic structure proposed above are the following: (i) the ground state is divided into many domains, (ii) each domain is long-range ordered and has a fixed value of $\phi$, (iii) the value of $\phi$ varies between different domains. A possible explanation for this magnetic structure is that $KCr_3(OD)_6(SO_4)_2$ is essentially an *XY*-spin system. In Eq. (1), the phase boundary between the two ground states (the $q=0$ structures with $+1$ chirality of $\phi=0°$ and 90°) resides at $E/D \simeq \sin^2\alpha/(1+\cos^2\alpha)$ and is nearly second order. At the boundary, hence the ground state energy becomes almost independent of $\phi$. We think $KCr_3(OD)_6(SO_4)_2$ is located near the phase boundary. Therefore the ground state is almost degenerated for all values of $\phi$, and thus the ordered moments can rotate about the *c* axis, keeping the 120° configuration. This spin fluctuation seems to be very slow because the broadening of the NMR spectrum was observed in the ordered phase.[12] The distribution of $\phi$ may not be uniform between 0° and 90°, and might be centered on the bottom of the shallow potential wells at $\phi=0°$ and 90°. The limit of this picture is a model where 50% of the crystal is $\phi=0°$ domain and the remainder is $\phi=90°$ domain, which also gives the same magnetic intensities as those of the uniform model. Consequently, $KCr_3(OD)_6(SO_4)_2$ is likely to be quite different from K jarosite. $KCr_3(OD)_6(SO_4)_2$ is representative of a kagomé lattice *XY*-spin antiferromagnet. Since the in-plane anisotropy is essentially zero, the $q=0$ ground state of $KCr_3(OD)_6(SO_4)_2$ is thought to be selected by in-plane[2] or interplane[8] further neighbor interactions, in contrast to K jarosite, where anisotropy is major force of choosing the ground state. Accordingly, the $q=0$ structure with $-1$ chirality can also be included in the ground states of $KCr_3(OD)_6(SO_4)_2$.

The idea that the ground state is slowly fluctuating might explain the difference between the previous results and ours. If the time scale of the fluctuations is quite short and is comparable to that of neutron scattering, the observed magnitude of the ordered moment becomes very small and the phase transition may be blurred, as seen in Ref. 8. It is interesting to point out that the lattice constant *c* of our sample at low temperature (17.11 Å) is significantly larger than the reported value 16.95 Å.[8] The lattice constants *c* of $KFe_3(OD)_6(SO_4)_2$ and $(D_3O)Fe_3(OD)_6(SO_4)_2$ are 17.12 (Ref. 5) and 16.90 Å,[15] respectively, hence the $K^+$ ion seems to expand the *c* axis more than the $D_3O^+$ ion. This implies that substitution of the $D_3O^+$ ion for the $K^+$ ion in our sample is small; the structural disorder is thought to be small in our sample. A structural disorder can break spin-spin correlation. A small domain is thought to fluctuate more rapidly than a large one, thus the disorder may promote the fluctuation. Actually, even for $T_N=2$ K samples, in a slow measurement such as $\mu$SR no long-range order is observed,[7] while small but finite ordered moments are found in a fast measurement such as neutron scattering.[8] This explanation possibly gives a unified view against different behaviors of various $KCr_3(OH)_6(SO_4)_2$.

## IV. CONCLUSION

The magnetic susceptibility and neutron powder diffraction measurements were carried out for the kagomé lattice antiferromagnet $KCr_3(OD)_6(SO_4)_2$ and it is found that the compound shows a definite indication of the long-range magnetic ordering, in contrast to the previous reports. The magnetic intensities of the ordered phase were well explained by a $q=0$ type 120° spin arrangement in which the direction of the moments varies from domain to domain. We think that subtle balance of the anisotropy terms makes $KCr_3(OD)_6(SO_4)_2$ equivalent to a kagomé lattice *XY*-spin antiferromagnet. We believe that our idea that the ground state is the $q=0$ structure fluctuating slowly around the *c* axis will be a key to understand the various experimental results obtained so far for $KCr_3(OH)_6(SO_4)_2$.

## ACKNOWLEDGMENTS

The authors would like to thank T. Osakabe, Y. Shimojo, K. Oikawa, and Professor K. Kakurai for their support in the neutron scattering experiments.

[1] J. N. Reimers and A. J. Berlinsky, Phys. Rev. B **48**, 9539 (1993).
[2] A. B. Harris, C. Kallin, and A. J. Berlinsky, Phys. Rev. B **45**, 2899 (1992).
[3] A. Chubukov, Phys. Rev. Lett. **69**, 832 (1992).
[4] J. T. Chalker, P. C. W. Holdsworth, and E. F. Shender, Phys. Rev. Lett. **68**, 855 (1992).
[5] T. Inami, M. Nishiyama, S. Maegawa, and Y. Oka, Phys. Rev. B **61**, 12 181 (2000).
[6] M. G. Townsend, G. Longworth, and E. Roudaut, Phys. Rev. B **33**, 4919 (1986).
[7] A. Keren, K. Kojima, L. P. Le, G. M. Luke, W. D. Wu, Y. J. Uemura, M. Takano, H. Dabkowska, and M. J. P. Gingras, Phys. Rev. B **53**, 6451 (1996).
[8] S.-H. Lee, C. Broholm, M. F. Collins, L. Heller, A. P. Ramirez, C. Kloc, E. Bucher, R. W. Erwin, and N. Lacevic, Phys. Rev. B **56**, 8091 (1997).
[9] F. Izumi, in *The Rietveld Method*, edited by R. A. Young (Oxford University Press, Oxford, 1993), Chap. 13.
[10] T. Inami, S. Maegawa, and M. Takano, J. Magn. Magn. Mater. **177-181**, 752 (1998).
[11] M. Nishiyama, T. Morimoto, S. Maegawa, T. Inami, and Y. Oka, Can. J. Phys. (to be published).
[12] T. Morimoto, M. Nishiyama, S. Maegawa, and Y. Oka (unpublished).
[13] C. L. Lengauer, G. Giester, and E. Irran, Powder Diffr. **9**, 265 (1994).
[14] J. A. Ripmeester, C. I. Ratcliffe, J. E. Dutrizac, and J. L. Jambor, Can. Mineral. **24**, 435 (1986).
[15] A. S. Wills, A. Harrison, S. A. M. Mentink, T. E. Mason, and Z. Tun, Europhys. Lett. **42**, 325 (1998).